

Phosphorus supply suppressed microbial necromass but stimulated plant lignin phenols accumulation in soils of alpine grassland on the Tibetan Plateau

Tian Ma^{a,b,1,*}, Zhiying Yang^{a,1}, Biwan Shi^a, Wenjing Gao^a, Yifan Li^a, Jianxiao Zhu^a, Jin-Sheng He^a

^a State Key Laboratory of Grassland and Agro-ecosystems, and College of Pastoral Agriculture Science and Technology, Lanzhou University, Lanzhou 730020, China

^b Observation and Research Station on Eco-environment of Frozen Ground in the Qilian Mountains, Lanzhou University, Lanzhou 730020, China

ARTICLE INFO

Handling Editor: Diego Abalos

Keywords:

Soil organic carbon
Microbial necromass
Lignin phenols
N and P addition
Alpine grassland

ABSTRACT

Increased nitrogen (N) and phosphorus (P) inputs have fundamental effects on the soil organic carbon (SOC) composition and dynamics. However, the responses of plant- and microbial-derived SOC components to N and P addition in alpine grasslands are poorly understood. Based on a 10-year N and P addition experiment conducted in the alpine grassland of the Tibetan Plateau, we used amino sugars and lignin phenols as tracers for microbial necromass and plant lignin components, respectively, and explored their accumulation with the addition of N and P. We found that P and N + P addition (P supply) decreased microbial necromass, whereas N addition did not have a significant effect. In comparison, the P supply increased lignin phenols in the topsoil, but N addition decreased them in the subsoil. Among these factors, soil total P played a non-negligible role in controlling the accumulation of amino sugars and lignin phenols in soils. In addition, decreased ratios of fungi-to-bacteria necromass carbon and amino sugars to lignin phenols were observed with P supply. This implies that although the 10-year P supply did not change the SOC significantly, it may have eventually increased the SOC loss potential. Collectively, we attempted to elucidate the underlying mechanisms of long-term SOC sequestration, which has important implications for plant- and microbial-mediated carbon processes in the context of increasing N and P inputs.

1. Introduction

Soil stores approximately 1500 Pg of carbon (C) with varied composition and structure in the top meter (Balesdent et al., 2018; Lal et al., 2021), more than the global vegetation and atmosphere combined (Lehmann and Kleber, 2015). Minor changes in soil organic carbon (SOC) profoundly influence atmospheric concentrations of greenhouse gases (Lehmann and Kleber, 2015). It has been proven that the SOC cycle is tightly interlinked with nitrogen (N) and phosphorus (P) cycles on molecular to global scales (Finzi et al., 2011). Globally prevalent N and P deposition can substantially influence SOC dynamics by regulating plant C inputs and microbial catabolism and anabolism (Finzi et al., 2011; Yue et al., 2017). Mounting evidence suggests that SOC accumulation largely depends on the relative contribution and

preservation of plant- and microbial-derived C components (Ma et al., 2018a; Cotrufo et al., 2019). Thus, understanding the SOC composition and accrual under increased N and P inputs through plant- and microbial-mediated mechanisms will be beneficial for addressing future climate change scenarios.

The N and P are two fundamental nutrients for plants in terrestrial ecosystems and are expected to trigger a net terrestrial C release into the atmosphere (Wieder et al., 2015). Increasing N and P inputs can potentially enhance plant growth and production, thereby increasing plant-derived C input and accumulation in soils (Li et al., 2016; Chenu et al., 2019). However, increased plant biomass may not lead to increased SOC storage (Jackson et al., 2017), because it depends on the relative contribution of plant input and microbial degradation (Angst et al., 2021). Increased plant-derived C input with synthetic fertilizers,

* Corresponding author at: State Key Laboratory of Grassland and Agro-ecosystems, and College of Pastoral Agriculture Science and Technology, Lanzhou University, Lanzhou 730020, China.

E-mail address: matian4022@126.com (T. Ma).

¹ Tian Ma and Zhiying Yang contributed equally to this work and should be considered co-first authors.

<https://doi.org/10.1016/j.geoderma.2023.116376>

Received 9 September 2022; Received in revised form 2 February 2023; Accepted 3 February 2023

Available online 8 February 2023

0016-7061/© 2023 The Author(s). Published by Elsevier B.V. This is an open access article under the CC BY-NC-ND license (<http://creativecommons.org/licenses/by-nc-nd/4.0/>).

including N, P, and potassium nutrients, can stimulate microbial proliferation and decomposition of plant substrates, leading to unchanged plant contributions to SOC in temperate agro-ecosystems (Li et al., 2020). However, the addition of N and P can also increase litter recalcitrance to microbial degradation (Angst et al., 2021; Ma et al., 2022), thereby promoting the preservation of plant-derived C in soils. These inconsistencies are likely to induce puzzling responses in plant-derived C to N and P addition, which warrant further in-depth study.

Microbial-derived C plays a more crucial role than plant-derived C in mediating SOC cycling and preservation (Liang et al., 2017; Ma et al., 2018a). Microbial-derived C tends to bind strongly to mineral surfaces because of its amphiphilicity compared with plant-derived C (Sollins et al., 2006; Kopittke et al., 2018). Microbes can also assimilate plant-derived C into microbial cells through *in vivo* pathways, which can further contribute to microbial biomass and accumulate in soils as relatively stable microbial residues and byproducts (Liang et al., 2017). Microbial necromass is a key component in controlling SOC storage and dynamics (Ma et al., 2018a; Zhu et al., 2020). It has been documented that microbial necromass can account for as much as > 50% of SOC in temperate agricultural (55.6%) and grassland (61.8%) soils (Liang et al., 2020; Bai and Cotrufo, 2022), and 70% of them are derived from fungal necromass (Wang et al., 2021). Recent studies have demonstrated that microbial necromass, particularly fungal necromass, is sensitive to nutrient addition in grasslands in the USA (Widdig et al., 2020), which may be attributed to their habitation in macroaggregates with weaker physical protection (Lützwow et al., 2006; Angst et al., 2021). Studies on the influence and main drivers of N and P addition on microbial necromass are inconsistent. For instance, N addition significantly promotes the accumulation of microbial necromass (mainly fungal necromass) owing to decreased N-acquisition enzyme activity with 4-year N and P addition in subtropical forests (Wang et al., 2022a, Wang et al., 2022b). In such cases, lower pH with N addition can also restrict enzyme diffusion (Tian and Niu, 2015; Chi et al., 2019; Wilpiszski et al., 2019), which appears to be the main driver of the increased accumulation of microbial necromass. In contrast, a *meta*-analysis reported inhibitory effects of N combined with P addition on microbial necromass in global forests (Hu et al., 2022). The aggravated microbial C limitation and N-acquisition enzyme activity were the two main reasons for the decreased microbial necromass (Hu et al., 2022). Therefore, studies exploring microbial necromass responses to N and P addition, and their corresponding mechanisms, are necessary.

As lignin phenols can exclusively be formed by higher plants, and amino sugars are found in microbial cell walls, they are widely used to represent plant- and microbial-derived SOC components, respectively (Joergensen, 2018; Thevenot et al., 2010). Both are thought to be major components of the stable SOC pool that affects long-term SOC sequestration (Liang et al., 2017; Thevenot et al., 2010). They can provide important information to illustrate the sources, compositions, and dynamics of the SOC (Table 1). Previous studies have shown that N addition does not significantly change lignin phenol content in temperate grassland soils (Crème et al., 2018). In comparison, N and P addition increases microbial necromass (Luo et al., 2020) in alpine grassland soils, but high N addition significantly decreases fungal necromass in grassland soils in Switzerland (Van Groenigen et al., 2007). However, few studies have investigated the effects of N and P addition on lignin phenols and amino sugars simultaneously in grassland soils. In particular, the fate of lignin phenols and amino sugars in alpine grassland soils with elevated N and P input is unclear.

As the largest plateau on Earth, the Tibetan Plateau has been subjected to significant climatic change and intensified human activities since the 1970s, which has had a striking impact on the biogeochemistry of this region (Chen et al., 2022). Atmospheric deposition and fertilizer application have substantially increased N and P inputs to the Tibetan Plateau (Peñuelas et al., 2013; Wang et al., 2022a, Wang et al., 2022b). As a crucial carbon stock with > 48Pg C estimated in the upper 1 m of soils (Mu et al., 2015), SOC dynamics may be profoundly influenced by

Table 1

Biomarkers used in this study and their biological and ecological significance.

Biomarkers	Molecular composition	Abbreviation	Parameter	Research implication
Lignin phenols	Vanillyl	V	(Ad/Al) _s	Indicating lignin oxidation stage in soils, with higher values mean higher oxidation stage
	Syringyl	S	(Ad/Al) _v	
	Cinnamyl	C	S/V, C/V	
Amino sugars	Glucosamine	GluN	GluN/ MurA	Indicating relative contribution of fungi and bacteria to the accumulation of SOC, with higher values mean more fungi-derived C in SOC
	Galactosamine	GalN		
	Muramic acid	MurA		
	Mannosamine	ManN		

increased exogenous N and P inputs. Hence, we examined the responses of plant- and microbial-derived SOC components to N and P addition in alpine grassland on the Tibetan Plateau. We aimed to (1) investigate the effects of N and P addition on plant- and microbial-derived SOC components in alpine grassland and (2) evaluate how N and P addition influences SOC sequestration and stabilization by combining plant biomass, soil properties, and microbial enzyme activities. We hypothesized that N and P addition may (1) not influence the accumulation of plant lignin components in soils because of the enhanced plant inputs and microbial degradation simultaneously and (2) increase the accumulation of microbial necromass along with enhanced microbial biomass.

2. Materials and methods

2.1. Site description and experimental design

The field experiments on N and P addition were conducted at the Haibei Alpine Grassland Ecosystem Research Station (37°29'–37°45' N, 101°12'–101°23' E; 3220 m above sea level), located in the northeast of the Tibetan Plateau in Qinghai Province, China. The climate is considered to be a typical continental monsoon with cold winters and warm summers. The mean annual temperature and precipitation were -1.2°C and 489 mm from 1980 to 2014, respectively (Liu et al., 2018), with 80% of precipitation occurring during the growing season from May to September. The soils at this site belong to the Mat-Gryic Cambisols, according to the IUSS Working Group World Reference Base for Soil Resources (WRB, 2015), with a clay loam texture, relatively high SOC concentrations of 6.3%, and a mean pH of 7.9 at 0–10 cm. The native plant species are dominated by *Kobresia humilis*, *Elymus nutans*, *Stipa aliena*, and *Gentiana straminea* (Jia et al., 2017).

The N and P addition experiment on the Tibetan Plateau was conducted in May 2011 based on a random block design ($n = 6$). Six treatments were included in each block: no addition (CK, Control), three levels of N addition (N1, 25 kg N ha⁻¹ yr⁻¹; N2, 50 kg N ha⁻¹ yr⁻¹; N3, 100 kg N ha⁻¹ yr⁻¹), P addition (P, 50 kg P ha⁻¹ yr⁻¹), and combined N and P addition (N + P, 100 kg N ha⁻¹ yr⁻¹ plus 50 kg P ha⁻¹ yr⁻¹). In total, there were 36 plots (6 m × 6 m) in six replicate blocks in this study. The widths of the buffer strips between the blocks and between the plots were 2 and 1 m, respectively. The applied fertilizers were urea for N fertilizer and triple superphosphate for P fertilizer, which were divided into three equal parts and evenly spread by hand onto the ground

surface after sunset, with high moisture levels and low temperatures at the beginning of June, July, and August during the annual growing season.

2.2. Plant and soil sampling

After nutrient addition, plant and soil samples were collected on 24 August 2020, from four selected treatments: CK (no addition), N (100 kg N ha⁻¹ yr⁻¹), P (50 kg P ha⁻¹ yr⁻¹), and N + P (100 kg N ha⁻¹ yr⁻¹ plus 50 kg P ha⁻¹ yr⁻¹). Nine species with the top 80% of shoot biomass were identified and collected from the four chosen treatments, and roots were sampled as mixed roots from the soil cores. Subsequently, shoots of different species and roots were mixed into a composite sample based on treatment. In three randomly selected replicates out of the six blocks, three cores of soil (topsoil, 0–10 cm and subsoil, 20–30 cm) were taken from each plot and mixed thoroughly to obtain one composite sample after removing grass, roots, and stones, and then passed through a 2-mm sieve. The sieved soil samples were immediately shipped to the laboratory on ice and were divided into two subsamples. One subsample was stored at 4 °C for the analysis of extracellular enzyme activities. The second subsample was freeze-dried at -50 °C to extract lignin phenols and amino sugars.

2.3. Soil property analysis

SOC and total nitrogen (TN) contents were quantified using an elemental analyzer (Elementar vario EL cube, Germany), with inorganic C removed using 1 M hydrochloric acid (HCl) before SOC measurement. Soil total P (TP) was extracted by digesting the samples in H₂SO₄-HClO₄ and was analyzed using an Auto Discrete chemical analyzer (AMS Smarchem450, Italy). Microbial biomass C (MBC) and N (MBN) were measured using the chloroform fumigation-extraction technique (Vance et al., 1987). Fumigated and non-fumigated soil samples were extracted with 0.5 M K₂SO₄ in a soil solution with a soil:water ratio of 1:4 (w:v). The filtered liquor was analyzed using a total organic carbon analyzer (Elementar Vario TOC, Germany). The organic carbon (OC) content of non-fumigated samples was defined as the dissolved OC (DOC) content. MBC and MBN were calculated as OC and N differences between fumigated and non-fumigated samples divided by a factor of 0.45 for MBC and 0.54 for MBN. Inorganic nitrogen (IN), including ammonium (NH₄⁺-N) and nitrate (NO₃⁻-N), was extracted with 2 M potassium chloride at a 1:10 soil:water ratio (w:v) using an Auto Discrete chemical analyzer (AMS Smarchem450, Italy). The soil texture was examined by laser diffraction using a Malvern Mastersizer 2000 (Malvern Instruments Ltd., UK). Soil pH was measured in a 1:2.5 soil:water (w:v) suspension with a pH meter.

2.4. Lignin phenols and amino sugars analysis

Lignin phenols in soils (top- and subsoils) and plants (shoots and roots) were extracted and quantified using the copper oxide (CuO) oxidation method (Feng and Simpson, 2007). Briefly, freeze-dried soil (2 g) or plant (50 mg) samples were mixed with 1 g of CuO, 100 mg of ammonium iron (II) sulfate hexahydrate [Fe (NH₄)₂(SO₄)₂·6H₂O], and 20 mL of nitrogen-purged NaOH solution (2 M) in Teflon-lined bombs. All the bombs were flushed with N₂ in the headspace for 10 min and heated at 150 °C for 2.5 h. After the heating, the bombs were cooled in running water. The liquid was decanted into a Teflon centrifuge tube (50 mL), and the residue was washed twice with 10 mL Milli-Q water using a rotary mixer for 10 min. After centrifugation (10 min at 2500 rpm), the supernatant was decanted into a fresh Teflon centrifuge tube (50 mL). The lignin oxidation products (LOPs) were spiked with a surrogate standard (ethyl vanillin), acidified to pH < 2 using 12 M HCl, and incubated for 1 h at room temperature in the dark to prevent cinnamic acid reactions. After centrifugation (30 min at 2500 rpm), LOPs were liquid-liquid extracted from the clear supernatant with ethyl acetate

three times, spiked with an internal standard (*trans*-cinnamic acid), and concentrated under N₂. The quantification of LOPs was based on derivatization using N, O-bis-(trimethylsilyl) trifluoroacetamide (BSTFA) and pyridine (70 °C, 3 h) to yield trimethylsilyl (TMS) derivatives.

Amino sugars were extracted from the freeze-dried soil following the classic method described by Zhang and Amelung (1996). Briefly, freeze-dried soil (0.5 g) was hydrolyzed with 10 mL of 6 M HCl at 105 °C for 8 h. Then, 100 µg of myo-inositol was injected into the cooled samples as a surrogate standard, which was filtered and dried via rotary evaporation at 50–53 °C under reduced pressure. The residues were re-dissolved in 5 mL of Milli-Q water and adjusted to pH 6.6–6.8 with 1 M potassium hydroxide. After discarding the precipitate by centrifugation, the supernatant was dried completely by rotary evaporation. The resultant residues were re-dissolved in absolute methanol and transferred to a vial to dry them under a gentle stream of N₂ at 45 °C. Amino sugars were re-dissolved in 1 mL Milli-Q water, with an additional 100 µg of recovery standard (*N*-methylglucamine), and subsequently freeze-dried overnight. The purified amino sugars were treated with 0.3 mL derivatization reagents (32 mg mL⁻¹ hydroxylamine hydrochloride and 40 mg mL⁻¹ 4-dimethylamino-pyridine in pyridine-methanol at a 4:1 vol ratio) at 75–80 °C for 30 min to obtain the aldonitrile derivatives. After cooling to room temperature, the derivatives were further acetylated with 1 mL of acetic anhydride at 75–80 °C for 20 min and mixed with 1.5 mL of dichloromethane. Excess derivatization reagents were thoroughly removed by extraction with HCl (1 M) and Milli-Q water. The amino sugar derivatives concentrated by N₂ were dissolved in 500 µL of a mixture of hexane and ethyl acetate solvent (v:v = 1:1) for analysis.

Biomarkers of interest were identified using a gas chromatograph (GC) coupled to a single quadrupole mass spectrometer (Shimadzu QP2020, Japan) with a DB-5 fused silica capillary column (30 m × 0.25 mm × 0.25 µm). The GC temperature program for lignin phenols was as follows: an initial column temperature of 65 °C was maintained for 2 min, and then the temperature was increased at 6 °C/min to 300 °C for 15 min. For amino sugars, the GC temperature program was as follows: an initial column temperature of 120 °C was held for 1 min, then the temperature was increased at 10 °C/min to 250 °C for 2.5 min, and then the temperature was increased again at 40 °C/min to 270 °C for 5.5 min. The mass spectra were compared with surrogate standards of typical lignin phenols to quantify the compounds and calculate the losses during the extraction procedures. External quantification standards were used to normalize the response factors for the different lignin phenols and amino sugars (Ma et al., 2018a).

The lignin phenol contents were calculated as the sum of vanillyl (V; vanillin, acetovanillone, vanillic acid), syringyl (S; syringaldehyde, acetosyringone, syringic acid), and cinnamyl (C; *p*-coumaric acid, ferulic acid) monomers (Ma et al., 2018a). The amino sugar contents refer to the sum of glucosamine, galactosamine, muramic acid, and mannosamine. Microbial necromass C was estimated using the following formula (Liang et al., 2019):

$$\text{Fungal necromass C} = (\text{glucosamine}/179.2 - 2 \times \text{muramic acid}/251.2) \times 179.2 \times 9 \quad (1)$$

$$\text{Bacterial necromass C} = \text{muramic acid} \times 45 \quad (2)$$

where 179.2 is the molecular weight of glucosamine, and 251.2 is the molecular weight of muramic acid, with an assumed 1:2 M ratio on average for muramic acid and glucosamine in bacterial cells. The average conversion coefficient of fungal glucosamine to fungal necromass C was 9 and the average conversion coefficient of bacterial muramic acid to bacterial necromass C was 45. Total microbial necromass C was calculated as the sum of fungal necromass C and bacterial necromass C.

2.5. Enzyme activity assay

Activities of AG (α -1,4-glucosidase), BG (β -1,4-glucosidase), NAG (β -1,4-*N*-acetyl-glucosaminidase), LAP (leucine aminopeptidase), AP (acid phosphatase), and PO (phenol oxidase) were measured according to the methods of Zhu et al. (2021). The specific substrates of the five hydrolases (AG, BG, NAG, LAP, and AP) used sodium acetate as a buffer (pH = 5), and the specific substrate of phenol oxidase (PO) used Tris as a buffer (50 mM). For each sample, fresh soil (1 g) and Milli-Q water (125 mL) were mixed into the soil slurry. For hydrolases, the synthetic substrates of AG, BG, AP, and NAG were fluorescently labeled with 4-methylumbelliferone (MUB), whereas only the synthetic substrate of LAP was fluorescently labeled with 7-amino-4-methylcoumarin (MUC). Standard curves for MUB and MUC were prepared for each sample using eight concentration gradients. The soil slurry (200 μ L) was pipetted into black 96-well microplates along with 50 μ L of 200 μ m enzyme substrate or 50 μ L of 200 μ m MUB or MUC for each replicate well for enzyme activities measurement and standard curves. Six replicates of each soil sample were incubated in black 96-well microplates at 25 °C for 4 h. For phenol oxidase (PO), 200 μ L of soil slurry and 50 μ L of 200 μ m enzyme substrate were pipetted into transparent 96-well microplates for each replicate. Sample background wells for each sample were pipetted into 200 μ L soil slurry and 50 μ L of 50 mM Tris buffer. The substrate and buffer background wells for each transparent 96-well microplate were pipetted into 200 μ L Milli-Q water and 50 μ L of enzyme substrate or Tris buffer, respectively. Eight replicates of each soil sample were incubated in transparent 96-well microplates at 25 °C for 3 h. Fluorescence was quantified by excitation at 365 nm and emission at 450 nm (hydrolytic enzymes), and the absorbance was measured at 450 nm (oxidative enzymes) using a microplate reader (Thermo Fisher Scientific, USA).

2.6. Data analysis

Before analysis, the normality test (Shapiro-Wilk test) showed that most of the variables were not normally distributed. Thus, all variables were log₁₀ transformed to achieve a normal distribution and the same order of magnitude. Differences in biomarker concentrations and related ratios of plants and soils were examined using one-way analysis of variance (ANOVA) among treatments and independent sample *t* test between the topsoil and subsoil. A two-way ANOVA was used to examine the main effects and their interactions within treatments and soil depths on the concentrations and related ratios of the biomarkers. The statistical analyses were performed using SPSS 24.0 (IBM SPSS Statistics 24.0, Chicago, IL). Redundancy analysis (RDA) was performed to visualize the correlations between lignin phenols, amino sugars and plant biomass, soil properties, microbial enzyme activities using 'vegan' package in R software (version 4.1.3). Pearson's regression analysis was used to assess the relationships between lignin phenols, amino sugars, and influencing factors, as well as between the two groups of biomarkers, using the R software (version 4.1.3). The random forest (RF) modeling analysis created in R ranked the investigated factors (soil properties and microbial enzyme activities) in the order of feature importance for explaining lignin phenols and amino sugars and identified the number of important factors using 10-fold cross-validation implemented with the 'rfcv()' function in the R package 'randomForest' with five repeats. The minimum cross-validation error was obtained when using six and eleven important factors for lignin phenols and amino sugars, respectively (Zhang et al., 2018). The relative importance of the variables was expressed as a percentage increase in the mean squared error (MSE), with higher MSE% values implying more important variables. The significance of each factor was further assessed with the 'rfrpermute' package in R software (version 4.1.3). The differences were considered statistically significant at $p < 0.05$.

3. Results

3.1. Lignin phenols in plants and soils

The OC-normalized concentrations of lignin phenols in aboveground plants ranged from 67.2 ± 1.6 to 78.7 ± 10.3 mg g⁻¹ OC, lower than those in belowground plants which ranged from 61.1 ± 13.5 to 175.3 ± 49.2 mg g⁻¹ OC ($p < 0.05$). The aboveground and belowground plants were insensitive to the addition of N and P ($p > 0.05$; Fig. 1a). Compared with CK, the S/V ratio decreased by 21.1% on average with P and N + P addition in aboveground plants, whereas no change was observed with N and P addition in belowground plants ($p > 0.05$; Fig. 1b). The ratios of (Ad/Al)_V and (Ad/Al)_S were in the range of 0.2 ± 0.01 – 0.3 ± 0.03 , and did not respond significantly to N and P addition, except for the decreased (Ad/Al)_S ratio with N + P addition in the aboveground plants ($p < 0.05$; Fig. 1c). A higher (Ad/Al)_V ratio was found belowground than aboveground plants, whereas the opposite was true for the (Ad/Al)_S ratio ($p < 0.05$; Fig. 1c).

The SOC-normalized concentrations of lignin phenols varied from 2.4 ± 0.3 to 4.9 ± 0.4 mg g⁻¹ SOC, and increased 1–2 times with P and N + P addition in the topsoil but decreased by 32.3% with N addition in the subsoil ($p < 0.05$; Fig. 2a). The lignin phenol monomers of V, S, and C shared similar concentrations of 0.8 ± 0.1 to 3.0 ± 0.2 mg g⁻¹ SOC among treatments in the top- and subsoils (Fig. 2b-d). All of these increased by 83.9–247.5% with P and N + P addition to the topsoil ($p < 0.05$) and decreased by 28.2–42.6% with N addition to the subsoil ($p < 0.05$).

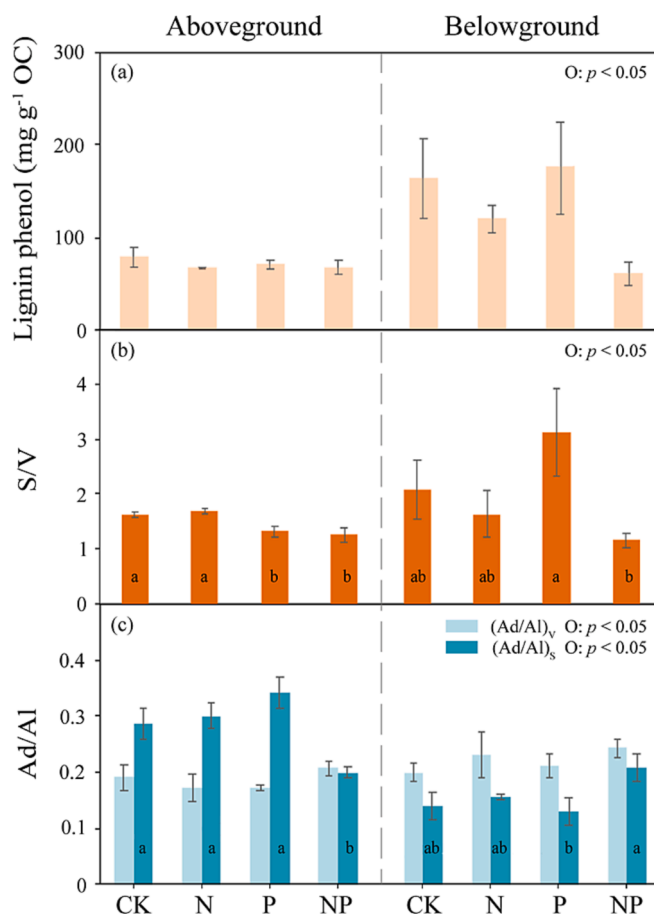
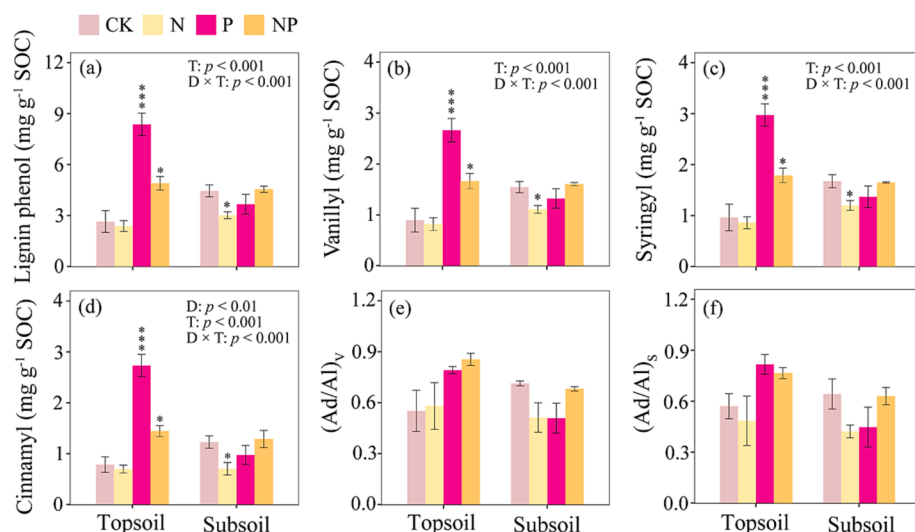


Fig. 1. Effects of nutrient addition on the OC-normalized concentrations of lignin phenols (a), the ratios of S/V (b), (Ad/Al)_S, and (Ad/Al)_V (c) in plants. The effects of plant organs (O, aboveground, and belowground plants) are shown. Bars indicate standard error (n = 3). Letters indicate the differences among treatments of aboveground and belowground plants. S, syringyl; V, vanillyl. CK, control; N, N addition; P, P addition; NP, N + P addition.



0.05; Fig. 2b-d). Nevertheless, the ratios of $(Ad/Al)_V$ and $(Ad/Al)_S$ showed no significant response to N and P addition in the top- and subsoils (Fig. 2e-f).

3.2. Amino sugars and microbial necromass in soils

The SOC-normalized concentrations of amino sugars were in the range of 32.2 ± 0.6 – 61.6 ± 2.5 $mg\ g^{-1}$ SOC with 29.5–47.7% lower under P and N + P addition relative to CK in the top- and subsoils ($p < 0.05$; Fig. 3a). Glucosamine was the most abundant component of the amino sugars, followed by galactosamine, which accounted for >95% of the total amino sugars (Fig. 3b-c). The concentrations of glucosamine and galactosamine decreased by 39.3% and 37.0% with P and N + P addition in the top- and subsoils, respectively ($p < 0.05$), which mainly contributed to the decreased concentrations of total amino sugars (Fig. 3a-c). However, the concentrations of muramic acid and mannosamine did not vary statistically with N and P addition in the topsoil or subsoil ($p > 0.05$; Fig. 3d-e). These results cooperatively resulted in an apparently decreased GluN/MurA ratio with the addition of P and N + P to the subsoil ($p < 0.05$; Fig. 3f). The GluN/MurA ratio was higher in the subsoil than in the topsoil ($p < 0.05$; Fig. 3f). However, N addition had no effect on amino sugars or other related parameters ($p > 0.05$; Fig. 3).

The SOC-normalized concentrations of microbial necromass C

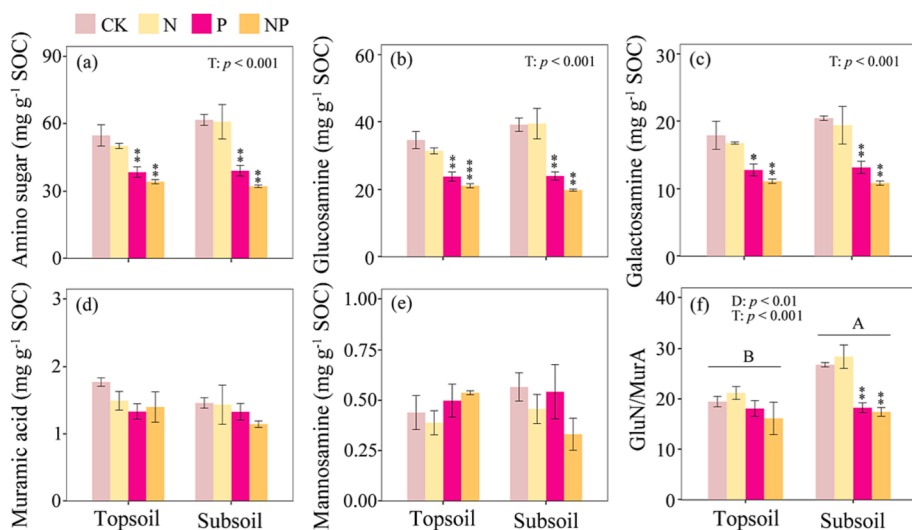


Fig. 2. Effects of nutrient addition on the SOC-normalized concentrations of lignin phenols (a-d) and the ratios of $(Ad/Al)_S$ and $(Ad/Al)_V$ (e-f) in soils. The effects of soil depth (D), nutrient addition treatments (T), and their interactions (D × T) are shown. Bars indicate standard error ($n = 3$). The absence of letters on the error bar indicates no significant difference between the topsoil and the subsoil. Asterisks denote significant differences between CK and nutrient addition treatments ($p < 0.05$). CK, control; N, N addition; P, P addition; NP, N + P addition. *, $p < 0.05$; ***, $p < 0.001$.

ranged from 215.6 ± 2.8 to 401.1 ± 50.2 $g\ kg^{-1}$ SOC, with fungal necromass C accounting for 78.5% on average (Fig. 4a-b). Both the total microbial necromass C and fungal necromass C decreased with P and N + P addition in the top- and subsoils ($p < 0.05$; Fig. 4a-b). No significant difference was found in bacterial necromass C among the treatments in the topsoil or subsoil (Fig. 4c). There was no change in the total microbial necromass C, fungal necromass C, or bacterial necromass C with N addition ($p > 0.05$; Fig. 4).

3.3. Ratios of fungi-to-bacteria necromass C and amino sugars to lignin phenols

The ratio of fungi-to-bacteria necromass C varied from 2.9 ± 0.6 to 5.4 ± 0.5 , obviously higher in the subsoil than that in the topsoil ($p < 0.05$; Fig. 5a). This ratio decreased with P and N + P addition in the subsoil ($p < 0.05$), but did not change in the topsoil ($p > 0.05$; Fig. 5a). The ratio of amino sugars to lignin phenols (AS/VSC) was in the range of 4.7 ± 0.6 – 23.7 ± 6.3 , with lower values with P addition in the topsoil and N + P addition in the top- and subsoils but higher values with N addition in the subsoil ($p < 0.05$; Fig. 5b).

Fig. 3. Effects of nutrient addition on the SOC-normalized concentrations of amino sugars (a-e) and GluN/MurA ratio (f). The effects of soil depth (D), nutrient addition treatments (T), and their interactions (D × T) are shown. Bars indicate standard error ($n = 3$). Bars with different capital letters are significantly different between the topsoil and the subsoil. Asterisks denote significant differences between CK and nutrient addition treatments ($p < 0.05$). MurA, muramic acid; GluN, glucosamine. CK, control; N, N addition; P, P addition; NP, N + P addition. **, $p < 0.01$; ***, $p < 0.001$.

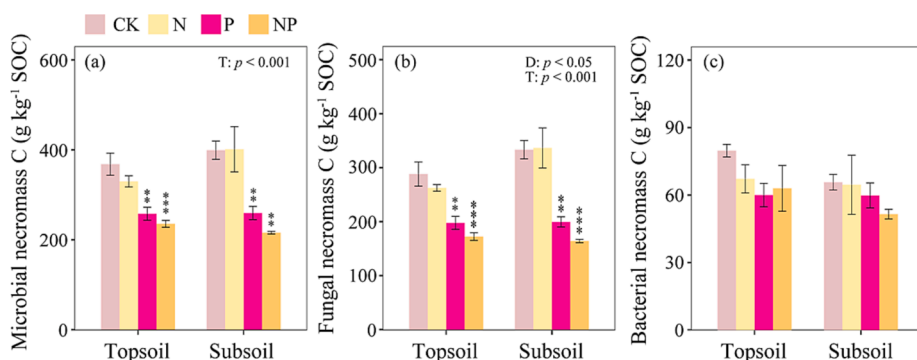


Fig. 4. Effects of nutrient addition on SOC-normalized concentrations of microbial necromass (a-c). The effects of soil depth (D), nutrient addition treatments (T), and their interactions (D × T) are shown. Bars indicate standard error (n = 3). The absence of letters on the error bar indicates no significant difference between the topsoil and the subsoil. Asterisks denote significant differences between CK and nutrient addition treatments ($p < 0.05$). CK, control; N, N addition; P, P addition; NP, N + P addition. **, $p < 0.01$; ***, $p < 0.001$.

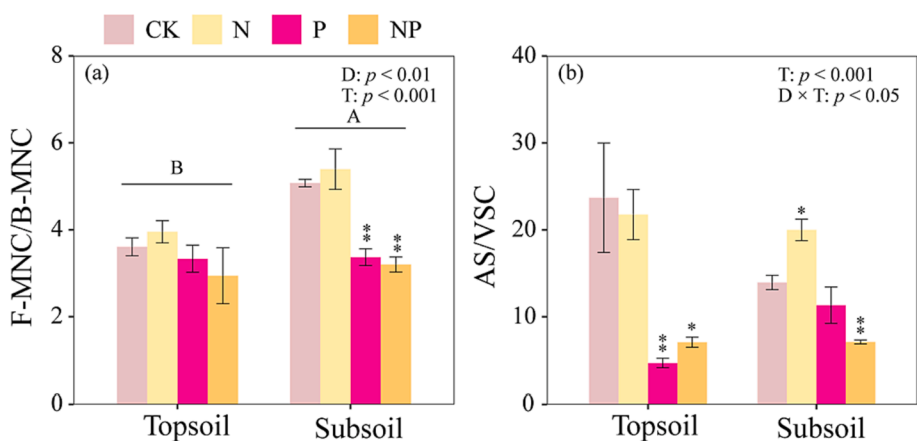


Fig. 5. Effects of nutrient addition on the ratio of fungi-to-bacteria necromass C (a), and the ratio of AS/VSC (b) in soils. The effects of soil depth (D), nutrient addition treatments (T), and their interactions (D × T) are shown. Bars indicate standard error (n = 3). The absence of letters on the error bar indicates no significant difference between the topsoil and the subsoil. Asterisks denote significant differences between CK and nutrient addition treatments ($p < 0.05$). AS, amino sugars; VSC, lignin phenols; F-MNC, fungal necromass C; B-MNC, bacterial necromass C. CK, control; N, N addition; P, P addition; NP, N + P addition. *, $p < 0.05$; **, $p < 0.01$.

3.4. Factors controlling lignin phenols and amino sugars

According to the RDA results, plant biomass, soil properties, and microbial enzyme activities played important roles in determining lignin

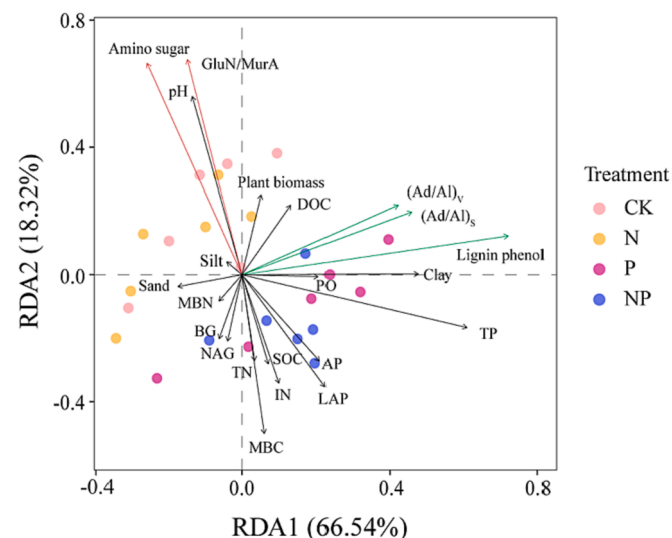


Fig. 6. Redundancy analysis (RDA) performed on two groups of biomarkers (green lines: lignin phenols; orange line: amino sugars) profiles and plant biomass, soil properties, and microbial enzyme activities (black lines) with N and P addition in the top- and subsoils. Arrows indicate correlations between biomarkers and plant biomass, soil properties, and microbial enzyme activities. Circles of different colors are used to distinguish the treatments. CK, control; N, N addition; P, P addition; NP, N + P addition.

phenols and amino sugars ($R^2 = 84.9\%$; Fig. 6). TP and pH, with the longest projections, had the most dominant effects on lignin phenols and amino sugars, followed by clay and MBC, respectively. Pearson's linear correlation analysis also revealed significant correlations between the lignin phenols ($r = 0.69$; Fig. S1), amino sugars ($r = -0.50$; Fig. S2), and TP. In addition, lignin phenols were negatively correlated with the ratios of SOC/TP and TN/TP, but positively correlated with clay (Fig.S1). Amino sugars showed negative correlations with the MBC/MBN ratio and LAP but positively correlated with pH (Fig. S2). The RF analysis was further performed to explore the dominant factors controlling the amino sugars and lignin phenols (Fig. 7). The RF model explained 54.75% and 45.92% of the variance in the lignin phenols and amino sugars, respectively. The relative importance ranking of the investigated factors (soil properties and microbial enzyme activities) revealed that TP was the most important factor for both biomarkers, followed by the ratios of TN/TP, SOC/TP, NAG, and AP for lignin phenols and the ratio of MBC/MBN for amino sugars ($p < 0.05$; Fig. 7).

4. Discussion

4.1. P supply suppressed the accumulation of microbial necromass in soils

The contribution of microbial necromass C to SOC in our study was similar to the 35.8–48.4% contribution in other alpine grassland soils (Ding et al., 2019), but lower than that in temperate grassland soils (Liang et al., 2019; Zhang et al., 2021). The inhibitory effects of low temperatures on plant production (Piao et al., 2006) and microbial growth, proliferation, and turnover (Chen et al., 2021; Zhang et al., 2021) impede microbial anabolism (Wang et al., 2020), which limits the accumulation of microbial necromass in alpine soils. Additionally, freeze–thaw events that occur on the Tibetan Plateau may lead to lower concentrations of amino sugars in soils (Sawicka et al., 2010; Jia et al.,

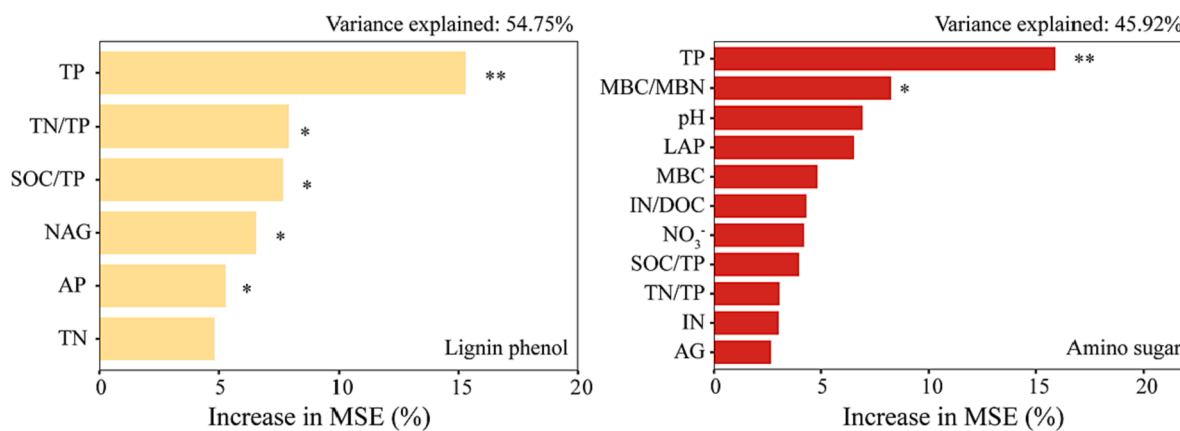


Fig. 7. Random forest (RF) mean predictor importance (percentage increase in mean square error) of lignin phenols (a) and amino sugars (b) among treatments in the top- and subsoils, showing factors with relative importance scores. The accuracy importance measure was computed for each tree and averaged over a forest (500 trees). The percentage increases in the mean squared error (MSE) of the variables were used to estimate the importance of these predictors; higher MSE% values imply more important predictors. *, $p < 0.05$; **, $p < 0.01$.

2021). Freeze-thaw events may accelerate the fragmentation and release of microbial cell walls into soils (Sawicka et al., 2010; Jia et al., 2021), further increasing the leaching loss and recycling of the microbial necromass (Nielsen et al., 2001; Matzner and Borken, 2008; Xu et al., 2018).

The accumulation of microbial necromass generally depends on the balance between the production and degradation of microbial metabolites (Joergensen, 2018). Inconsistent with our hypothesis, we found significantly decreased microbial necromass C with 10-year P and N + P addition (P supply; Fig. 4). Contrary to our results, Luo et al. (2020) found significantly increased microbial necromass due to a decrease in SOC with a 4-year P supply in the same field experiment. However, our results are consistent with those of Yuan et al. (2021), who also found significantly decreased microbial necromass with a 10-year P addition in a tropical forest. They suggested that the increased C- (BG) and N-acquisition enzyme (NAG) activities caused by P addition enhanced the degradation of the microbial necromass and hampered its accumulation. We also detected stimulated C- (AG and BG) and N-acquisition enzyme (LAP) activities with N + P addition in the topsoil and P addition in the subsoil, respectively (Fig. S3a-c). A negative correlation was observed between LAP and microbial necromass in the subsoil (Fig. S4d), implying that the increased degradation of microbial necromass might have contributed to the decrease in microbial necromass with P addition. Nevertheless, P supply did not decrease MBC in the top- and subsoils (Fig. S3d), which was combined with an insignificant correlation between MBC and amino sugars (Fig. S2), and ruled out the effect of microbial production on the reduced microbial necromass. In addition to increased enzyme activities, mineral protection largely influences the recycling of microbial necromass (Lützwow et al., 2006; Sollins et al., 2006). When microbial necromass is desorbed from mineral surface, it is more easily degraded and reutilized by microorganisms (Cui et al., 2020; Cai et al., 2022). In our study, the P supply introduced a considerable amount of competing phosphate ions into the topsoil (Table S1), because phosphate can bridge two or more metals on the mineral surface to form bi- or multinuclear surface complexes that block sorption sites for microbial necromass (Stumm, 1997; Mikutta et al., 2011; Kleber et al., 2015). This can markedly decrease the amount of microbial necromass adsorbed onto mineral surfaces (Alliot et al., 2005; Gasser et al., 2008; Hiemstra et al., 2010; Hiemstra, 2013), and increase the possibility of degradation and reutilization.

Moreover, microbial necromass is considered an N-enriched organic substrate (Liang et al., 2019), and the N restriction caused by P supply (Table S2) may accelerate the decomposition of microbial necromass to obtain N for microorganisms. Furthermore, the local charge disequilibrium encouraged by the depletion of desorbed microbial necromass stimulates the continuous release of microbial necromass from mineral-

organic-associated complexes into desorbed phases over longer time-scales (Kleber et al., 2015). Finally, the decrease in soil pH with P supply ($p < 0.05$; Table S1) may also drive the decline in microbial necromass. Minerals tend to dissolve at low pH (Blume et al., 2015), reducing their capacity to stabilize microbial necromass (Angst et al., 2021), and resulting in more unprotected microbial necromass that can be easily reutilized under N deficiency caused by P supply (Lützwow et al., 2006). The positive correlation between the microbial necromass and pH also supports this view (Fig. S4h). Taken together, the decrease in microbial necromass with P supply may be associated with increased decomposition, implying the potential role of mineral protection affected by P and soil pH in determining the accumulation of microbial necromass in soils.

It is worth mentioning that the decreased microbial necromass was mainly derived from fungal necromass with P supply. Ding et al. (2019) also found that a significant increase in fungal necromass, but not bacterial necromass, induced changes in total microbial necromass after 3-year warming in an alpine meadow. This indicates that fungi are more responsive to changing environments, given their preferential habitation in macroaggregates with weak physical protection (Lützwow et al., 2006; Ding et al., 2019). Additionally, fungal necromass with a broad range of SOC/TN ratios (Kallenbach et al., 2016) can meet the microbial stoichiometric demand (Cui et al., 2020) at different levels of C and N limitation; thus, more fungal necromass was degraded with P supply (Fig. 4b). This result conflicted with that of a 7-year nutrient addition experiment that found decreased fungal residues because of decreased fungal biomass with N addition in an N-saturated tropical forest (Ma et al., 2020). However, N constraint is common in our study area (Chen et al., 2022), and P supply exacerbates the N demand of microorganisms (Table S2; Vitousek et al., 2010; He and Dijkstra, 2015). Therefore, the aggravated N restriction resulting from the P supply led to the asynchronous decomposition of microbial necromass components because of their possibly different intrinsic stabilities (He et al., 2011), eventually altering the contribution of fungal and bacterial necromass (Ma et al., 2018b).

4.2. P supply stimulated the accumulation of plant lignin components in soils

The SOC-normalized concentrations of lignin phenols were 2.4 ± 0.3 – 8.4 ± 0.7 mg g⁻¹ SOC on average (Fig. 2a), which were in a lower range of 1.7–30.3 mg g⁻¹ SOC in alpine grassland soils (Zhu et al., 2019; Dai et al., 2022), whereas lower than 10–25 mg g⁻¹ SOC in subtropical forest soils (Wang et al., 2022a, Wang et al., 2022b). Surprisingly, we found that contrary to microbial necromass and our hypothesis, P supply remarkably increased the concentration of lignin phenols in the topsoil,

whereas N addition decreased it in the subsoil ($p < 0.05$; Fig. 2a). The increased concentrations of lignin phenols were the result of increased V, S, and C monomers with P supply to the topsoil (Fig. 2a-d). Previous studies have reported that the concentrations of lignin phenols increase in warmed soils which are associated with the suppression of lignin oxidation (Ma et al., 2022). However, we observed unaffected ratios of $(Ad/Al)_S$ and $(Ad/Al)_V$ with N and P addition (Fig. 2e-f), indicating that the preferentially accumulated lignin phenols were unrelated to microbial degradation. Conversely, decreased lignin phenols were found with P addition, along with unaffected $(Ad/Al)_S$ and $(Ad/Al)_V$ in a subalpine forest (Luo et al., 2022). They attributed the decreased lignin phenols to a greater reduction in C input from fine roots and the nuanced alteration of microbial community functions (Luo et al., 2022). By comparison, we excluded the influence of plant inputs, as no significant changes in plant lignin phenols and no increase in plant biomass were found with P supply (Fig. 1a and S6). However, P supply significantly decreased the S/V ratio of aboveground plant materials (Fig. 1b), indicating an improved chemical recalcitrance of plant substrates (Otto and Simpson, 2006; Clemente et al., 2011). Therefore, the enhanced concentrations of lignin phenols may originate from increased chemical recalcitrance and preferential accumulation with P supply in the topsoil. In addition, the degradation of lignin phenols is associated with the availability of labile C compounds, which are C and energy sources for microbial proliferation and use of organic matter (Frey et al., 2008; Cui et al., 2016; Ma et al., 2022). The N addition alleviated the C limitation of microorganisms in the subsoil (indicated by decreased vector length; $p < 0.05$; Table S2); thus, lignin phenols were decomposed as C sources by microorganisms. Together, these findings conjointly contribute to the selective retention of plant lignin components in soils.

4.3. Implications of N and P addition on SOC sequestration in alpine grassland

The 10-year P supply significantly increased lignin phenols in the topsoil, but decreased amino sugars in both the top- and subsoils (Figs. 2-3), which did not match the change in SOC (Table S1). The accumulation of SOC was fundamentally determined by the balance between organic matter inputs (i.e., plant residues) and losses (i.e., microbial decomposition) (Six et al., 2006). In our study, amino sugars and lignin phenols in soils constitute 3.2–6.2% and 0.2–0.8% of SOC, respectively (Figs. 2-3). These two groups of SOC components were probably inadequate to specify the overall SOC changes, as recently reported by Whalen et al. (2022). Therefore, separate or combined amino sugars and lignin phenols are inaccurate indicators of SOC dynamics in the context of N and P addition in alpine grasslands of the Tibetan Plateau. However, their feedback to N and P addition may indicate SOC stability, because they represent stable SOC components from microorganisms and plants, respectively.

As tracers of microbial necromass, amino sugars are typically made up of > 90% fungal and bacterial populations (Six et al., 2006). As discussed above (see section 4.1), the imbalanced soil stoichiometric ratio led to varied degrees of decreased fungal necromass and bacterial necromass, and generated a prominent decline in the fungi-to-bacteria necromass C ratio with P supply in the subsoil ($p < 0.05$; Fig. 5a). The ratio of fungi-to-bacteria necromass C had an average value of 3.9 in the top- and subsoils, at the high end of 1.2–4.1, which has recently been reported for global grasslands (Bai and Cotrufo, 2022). Previous evidence suggests that the ratio of fungi-to-bacteria necromass C ranges from 2.0 to 4.0 in forests globally (Ni et al., 2020; Luo et al., 2022). This result is at odds with the idea that fungal necromass contributes more to microbial necromass in forest soils than in grassland soils (Wang et al., 2021). Because fungal necromass is more chemically recalcitrant than bacterial necromass (Martin and Haider, 1979; Simpson et al., 2004; Joergensen, 2018), this ratio can be used to evaluate the stability of microbial necromass (Amelung, 2001; Six et al., 2006; Ma et al., 2018b). Consequently, the significantly decreased ratio of fungi-to-bacteria

necromass C in the subsoil resulting from decreased fungal necromass but constant bacterial necromass with P supply (Figs. 4-5) implies less stable microbial-derived C in the future.

The long-term build-up of the SOC pool is regulated by the retention of microbial and plant products in soils (Li et al., 2020). In our study, amino sugars played a more important role than lignin phenols in the formation of stable SOC, as reflected in two aspects: (1) the SOC-normalized concentrations of amino sugars were 20 times higher than those of lignin phenols (Figs. 2-3); and (2) the preferential degradation of amino sugars resulted in the concomitant retention of lignin phenols. Several studies have shown that stable SOC usually comprises more microbial compounds than plant constituents despite their high molecular stability (Lützwow et al., 2006; Thevenot et al., 2010; Zhu et al., 2020). Therefore, the AS/VSC ratio may be indicative of the SOC stability to some extent. As a result, the significantly decreased AS/VSC ratio with 10-year P supply in soils may indicate decreased SOC stability. In general, both decreased fungi-to-bacteria necromass C and AS/VSC ratios with a 10-year P supply point to a higher SOC loss potential in the future, and the composition and stability of SOC with increased N and P inputs warrant more attention.

5. Conclusions

A continuous P supply suppressed the accumulation of microbial necromass, whereas N addition did not significantly alter it. In comparison, the P supply enhanced lignin phenols in the topsoil, but N addition decreased them in the subsoil. With continuous P supply, the enhanced degradation of microbial necromass due to weakened mineral protection results in reduced microbial necromass, whereas the increased recalcitrance of plant lignin components leads to their selective retention in soils. TP is a vital factor that affects the accumulation of amino sugars and lignin phenols in soils. Furthermore, P supply reduced the relative stability of microbial necromass and SOC in soils, tending to increase SOC loss in the future. In brief, our study facilitates an accurate understanding of the complex SOC response to increased N and P inputs from plant lignin components and microbial necromass biomarker perspectives in the alpine grasslands of the Tibetan Plateau.

Declaration of Competing Interest

The authors declare that they have no known competing financial interests or personal relationships that could have appeared to influence the work reported in this paper.

Data availability

Data will be made available on request.

Acknowledgments

This study was supported by the Natural Science Foundation of Gansu Province (21JR7RA500) and Lanzhou University's "Double First-Class Initiative" Guided Project Team Building-Funding-Research Startup Fee (561119221). We are grateful to the Haibei National Field Research Station in the Alpine Grassland Ecosystem for maintaining the experimental platform. We would like to thank KetengEdit (www.ketengedit.com) for linguistic assistance during the preparation of this manuscript.

Appendix A. Supplementary data

Supplementary data to this article can be found online at <https://doi.org/10.1016/j.geoderma.2023.116376>.

References

- Alliot, C., Bion, L., Mercier, F., Toulhoat, P., 2005. Sorption of aqueous carbonic, acetic, and oxalic acids onto α -alumina. *J. Colloid Interface Sci.* 287 (2), 444–451.
- Amelung, W., 2001. Methods using amino sugars as markers for microbial residues in soil. In: *Assessment Methods for Soil Carbon*. Lewis Publishers Boca Raton, pp. 233–270.
- Angst, G., Mueller, K.E., Nierop, K.G.J., Simpson, M.J., 2021. Plant- or microbial-derived? A review on the molecular composition of stabilized soil organic matter. *Soil Biol. Biochem.* 156, 108189.
- Bai, Y., Cotrufo, M.F., 2022. Grassland soil carbon sequestration: Current understanding, challenges, and solutions. *Science* 377 (6606), 603–608.
- Balesdent, J., Basile-Doelsch, I., Chadoeuf, J., Cornu, S., Derrien, D., Fekiacova, Z., Hatté, C., 2018. Atmosphere-soil carbon transfer as a function of soil depth. *Nature* 559 (7715), 599–602.
- Blume, H.-P., Fleige, H., Horn, R., Kandeler, E., Kögel-Knabner, I., Kretzschmar, R., Stahr, K., Wilke, B.-M., 2015. *Soil Science*, first ed. Springer, Berlin Heidelberg, Berlin Heidelberg.
- Cai, Y., Ma, T., Wang, Y.Y., Jia, J., Jia, Y.F., Liang, C., Feng, X.J., 2022. Assessing the accumulation efficiency of various microbial carbon components in soils of different minerals. *Geoderma* 407, 115562.
- Chen, X., Hu, Y., Xia, Y., Zheng, S., Ma, C., Rui, Y., He, H., Huang, D., Zhang, Z., Ge, T., Wu, J., Guggenberger, G., Kuzyakov, Y., Su, Y., 2021. Contrasting pathways of carbon sequestration in paddy and upland soils. *Global Change Biol.* 27 (11), 2478–2490.
- Chen, H., Ju, P., Zhu, Q., Xu, X., Wu, N., Gao, Y., Feng, X., Tian, J., Niu, S., Zhang, Y., Peng, C., Wang, Y., 2022. Carbon and nitrogen cycling on the Qinghai-Tibetan Plateau. *Nat. Rev. Earth Environ.* 3, 701–716.
- Chenu, C., Angers, D.A., Barre, P., Derrien, D., Arrauays, D., Balesdent, J., 2019. Increasing organic stocks in agricultural soils: Knowledge gaps and potential innovations. *Soil Tillage Res.* 188, 41–52.
- Chi, J., Zhang, W., Wang, L., Putnis, C.V., 2019. Direct observations of the occlusion of soil organic matter within calcite. *Environ. Sci. Technol.* 53 (14), 8097–8104.
- Clemente, J.S., Simpson, A.J., Simpson, M.J., 2011. Association of specific organic matter compounds in size fractions of soils under different environmental controls. *Org. Geochem.* 42 (10), 1169–1180.
- Cotrufo, M.F., Ranalli, M.G., Haddji, M.L., Six, J., Lugato, E., 2019. Soil carbon storage informed by particulate and mineral-associated organic matter. *Nat. Geosci.* 12 (12), 989–994.
- Crème, A., Rumpel, C., Le Roux, X., Romian, A., Lan, T., Chabbi, A., 2018. Ley grassland under temperate climate had a legacy effect on soil organic matter quantity, biogeochemical signature and microbial activities. *Soil Biol. Biochem.* 122, 203–210.
- Cui, L.F., Liang, C., Duncan, D.S., Bao, X.L., Xie, H.T., He, H.B., Wickings, K., Zhang, X.D., Chen, F.S., 2016. Impacts of vegetation type and climatic zone on neutral sugar distribution in natural forest soils. *Geoderma* 282, 139–146.
- Cui, J., Zhu, Z.K., Xu, X.L., Liu, S.L., Jones, D.L., Kuzyakov, Y., Shibistova, O., Wu, J.S., Ge, T.D., 2020. Carbon and nitrogen recycling from microbial necromass to cope with C:N stoichiometric imbalance by priming. *Soil Biol. Biochem.* 142, 107720.
- Dai, G.H., Zhu, S.S., Cai, Y., Zhu, E.R., Jia, Y.F., Ji, C.J., Tang, Z.Y., Fang, J.Y., Feng, X.J., 2022. Plant-derived lipids play a crucial role in forest soil carbon accumulation. *Soil Biol. Biochem.* 168.
- Ding, X.L., Chen, S.Y., Zhang, B., Liang, C., He, H.B., Horwath, W.R., 2019. Warming increases microbial residue contribution to soil organic carbon in an alpine meadow. *Soil Biol. Biochem.* 135, 13–19.
- Feng, X., Simpson, M.J., 2007. The distribution and degradation of biomarkers in Alberta grassland soil profiles. *Org. Geochem.* 38 (9), 1558–1570.
- Finzi, A.C., Austin, A.T., Cleland, E.E., Frey, S.D., Houlton, B.Z., Wallenstein, M.D., 2011. Responses and feedbacks of coupled biogeochemical cycles to climate change: examples from terrestrial ecosystems. *Front. Ecol. Environ.* 9 (1), 61–67.
- Frey, S.D., Drijber, R., Smith, H., Melillo, J., 2008. Microbial biomass, functional capacity, and community structure after 12 years of soil warming. *Soil Biol. Biochem.* 40 (11), 2904–2907.
- Gasser, M.S., Mohsen, H.T., Aly, H.F., 2008. Humic acid adsorption onto Mg/Fe layered double hydroxide. *Colloids Surf. A* 331 (3), 195–201.
- He, M.Z., Dijkstra, F.A., 2015. Phosphorus addition enhances loss of nitrogen in a phosphorus-poor soil. *Soil Biol. Biochem.* 82, 99–106.
- He, H., Zhang, W., Zhang, X., Xie, H., Zhuang, J., 2011. Temporal responses of soil microorganisms to substrate addition as indicated by amino sugar differentiation. *Soil Biol. Biochem.* 43 (6), 1155–1161.
- Hiemstra, T., 2013. Surface and mineral structure of ferrihydrite. *Geochim. Cosmochim. Acta* 105, 316–325.
- Hiemstra, T., Antelo, J., van Rotterdam, A.M.D., van Riemsdijk, W.H., 2010. Nanoparticles in natural systems II: The natural oxide fraction at interaction with natural organic matter and phosphate. *Geochim. Cosmochim. Acta* 74 (1), 59–69.
- Hu, J.X., Huang, C.D., Zhou, S.X., Liu, X., Dijkstra, F.A., 2022. Nitrogen addition increases microbial necromass in croplands and bacterial necromass in forests: A global meta-analysis. *Soil Biol. Biochem.* 165, 108500.
- Jackson, R.B., Lajtha, K., Crow, S.E., Hugelius, G., Kramer, M.G., Piñeiro, G., 2017. The Ecology of Soil Carbon: Pools, Vulnerabilities, and Biotic and Abiotic Controls. *Annu. Rev. Ecol. Syst.* 48 (1), 419–445.
- Jia, J., Feng, X.J., He, J.S., He, H.B., Lin, L., Liu, Z.G., 2017. Comparing microbial carbon sequestration and priming in the subsoil versus topsoil of a Qinghai-Tibetan alpine grassland. *Soil Biol. Biochem.* 104, 141–151.
- Jia, D., Liu, M., Li, K., Wang, X., Wang, Z., Wen, J., Lai, X., 2021. Variations in the top-layer soil freezing/thawing process from 2009 to 2018 in the Maqu area of the Tibetan Plateau. *Theor. Appl. Climatol.* 143 (1–2), 21–32.
- Joergensen, R.G., 2018. Amino sugars as specific indices for fungal and bacterial residues in soil. *Biol. Fertil. Soils* 54, 559–568.
- Kallenbach, C.M., Frey, S.D., Grandy, A.S., 2016. Direct evidence for microbial-derived soil organic matter formation and its ecophysiological controls. *Nat. Commun.* 7, 1–10.
- Kleber, M., Eusterhues, K., Keiluweit, M., Mikutta, C., Mikutta, R., Nico, P.S., 2015. Mineral-organic associations: formation, properties, and relevance in soil environments. In: Sparks, D.L. (Ed.), *Advances in Agronomy*, pp. 1–140.
- Kopittke, P.M., Hernandez-Soriano, M.C., Dalal, R.C., Finn, D., Menzies, N.W., Hoeschen, C., Mueller, C.W., 2018. Nitrogen-rich microbial products provide new organo-mineral associations for the stabilization of soil organic matter. *Global Change Biol.* 24, 1762–1770.
- Lal, R., Mønger, C., Nave, L., Smith, P., 2021. The role of soil in regulation of climate. *Phil. Trans. R. Soc. B* 376, 20210084.
- Lehmann, J., Kleber, M., 2015. The contentious nature of soil organic matter. *Nature* 528, 60–68.
- Li, Y., Niu, S.L., Yu, G.R., 2016. Aggravated phosphorus limitation on biomass production under increasing nitrogen loading: a meta-analysis. *Global Change Biol.* 22, 934–943.
- Li, J., Zhang, X.C., Luo, J.F., Lindsey, S., Zhou, F., Xie, H.T., Li, Y., Zhu, P., Wang, L.C., Shi, Y.L., He, H.B., Zhang, X.D., 2020. Differential accumulation of microbial necromass and plant lignin in synthetic versus organic fertilizer-amended soil. *Soil Biol. Biochem.* 149, 107967.
- Liang, C., Schimel, J.P., Jastrow, J.D., 2017. The importance of anabolism in microbial control over soil carbon storage. *Nat. Microbiol.* 2, 1–6.
- Liang, C., Amelung, W., Lehmann, J., Kastner, M., 2019. Quantitative assessment of microbial necromass contribution to soil organic matter. *Global Change Biol.* 25, 3578–3590.
- Liang, X., Zhang, T., Lu, X., Ellsworth, D.S., BassiriRad, H., You, C., Wang, D., He, P., Deng, Q., Liu, H., Mo, J., Ye, Q., 2020. Global response patterns of plant photosynthesis to nitrogen addition: A meta-analysis. *Global Change Biol.* 26, 3585–3600.
- Liu, H.Y., Mi, Z.R., Lin, L., Wang, Y.H., Zhang, Z.H., Zhang, F.W., Wang, H., Liu, L.L., Zhu, B.A., Cao, G.M., Zhao, X.Q., Sanders, N.J., Classen, A.T., Reich, P.B., He, J.S., 2018. Shifting plant species composition in response to climate change stabilizes grassland primary production. *Proc. Natl. Acad. Sci. U. S. A.* 115, 4051–4056.
- Luo, R.Y., Kuzyakov, Y., Liu, D.Y., Fan, J.L., Luo, J.F., Lindsey, S., He, J.S., Ding, W.X., 2020. Nutrient addition reduces carbon sequestration in a Tibetan grassland soil: Disentangling microbial and physical controls. *Soil Biol. Biochem.* 144, 107764.
- Luo, R.Y., Kuzyakov, Y., Zhu, B., Qiang, W., Zhang, Y., Pang, X.Y., 2022. Phosphorus addition decreases plant lignin but increases microbial necromass contribution to soil organic carbon in a subalpine forest. *Global Change Biol.* 28, 4194–4210.
- Lüttow, M.V., Kögel-Knabner, I., Ekschmitt, K., Matzner, E., Guggenberger, G., Marschner, B., Flessa, H., 2006. Stabilization of organic matter in temperate soils: mechanisms and their relevance under different soil conditions - a review. *Eur. J. Soil Sci.* 57, 426–445.
- Ma, S.H., Chen, G.P., Tian, D., Du, E.Z., Xiao, W., Jiang, L., Zhou, Z., Zhu, J.L., He, H.B., Zhu, B., Fang, J.Y., 2020. Effects of seven-year nitrogen and phosphorus additions on soil microbial community structures and residues in a tropical forest in Hainan Island, China. *Geoderma* 361, 114034.
- Ma, L., Ju, Z., Fang, Y., Vancov, T., Gao, Q., Wu, D., Zhang, A., Wang, Y., Hu, C., Wu, W., Du, Z., 2022. Soil warming and nitrogen addition facilitates lignin and microbial residues accrual in temperate agroecosystems. *Soil Biol. Biochem.* 170, 108693.
- Ma, Z.Q., Zhang, X.Y., Zhang, C., Wang, H.M., Chen, F.S., Fu, X.L., Fang, X.M., Sun, X.M., Lei, Q.L., 2018b. Accumulation of residual soil microbial carbon in Chinese fir plantation soils after nitrogen and phosphorus additions. *J. For. Res.* 29, 953–962.
- Ma, T., Zhu, S.S., Wang, Z.H., Chen, D.M., Dai, G.H., Feng, B.W., Su, X.Y., Hu, H.F., Li, K.H., Han, W.X., Liang, C., Bai, Y.F., Feng, X.J., 2018a. Divergent accumulation of microbial necromass and plant lignin components in grassland soils. *Nat. Commun.* 9, 1–9.
- Martin, J.P., Haider, K., 1979. Biodegradation of ^{14}C -labeled model and cornstarch lignins, phenols, model phenolase humic polymers, and fungal melanins as influenced by a readily available carbon source and soil. *Appl. Environ. Microbiol.* 38, 283–289.
- Matzner, E., Borken, W., 2008. Do freeze-thaw events enhance C and N losses from soils of different ecosystems? A review. *Eur. J. Soil Sci.* 59, 274–284.
- Mikutta, R., Zang, U., Chorover, J., Haumaier, L., Kalbitz, K., 2011. Stabilization of extracellular polymeric substances (*Bacillus subtilis*) by adsorption to and coprecipitation with Al forms. *Geochim. Cosmochim. Acta* 75, 3135–3154.
- Mu, C., Zhang, T., Wu, Q., Peng, X., Cao, B., Zhang, X., Cao, B., Cheng, G., 2015. Editorial: Organic carbon pools in permafrost regions on the Qinghai-Xizang (Tibetan) Plateau. *Cryosphere* 9, 479–486.
- Ni, X.Y., Liao, S., Tan, S.Y., Peng, Y., Wang, D.Y., Yue, K., Wu, F.Z., Yang, Y.S., 2020. The vertical distribution and control of microbial necromass carbon in forest soils. *Glob. Ecol. Biogeogr.* 29, 1829–1839.
- Nielsen, C.B., Groffman, P.M., Hamburg, S.P., Driscoll, C.T., Fahey, T.J., Hardy, J.P., 2001. Freezing Effects on Carbon and Nitrogen Cycling in Northern Hardwood Forest Soils. *Soil Sci. Soc. Am. J.* 65, 1723–1730.
- Otto, A., Simpson, M.J., 2006. Evaluation of CuO oxidation parameters for determining the source and stage of lignin degradation in soil. *Biogeochemistry* 80, 121–142.
- Peñuelas, J., Poulter, B., Sardans, J., Ciais, P., van der Velde, M., Bopp, L., Boucher, O., Godderis, Y., Hinsinger, P., Llusia, J., Nardin, E., Vicca, S., Obersteiner, M., Janssens, I.A., 2013. Human-induced nitrogen-phosphorus imbalances alter natural and managed ecosystems across the globe. *Nat. Commun.* 4, 2934.
- Piao, S.L., Fang, J.Y., He, J.S., 2006. Variations in vegetation net primary production in the Qinghai-Xizang Plateau, China, from 1982 to 1999. *Clim. Change* 74, 253–267.

- Sawicka, J.E., Robador, A., Hubert, C., Jorgensen, B.B., Bruchert, V., 2010. Effects of freeze-thaw cycles on anaerobic microbial processes in an Arctic intertidal mud flat. *ISME J.* 4, 585–594.
- Simpson, R.T., Frey, S.D., Six, J., Thiet, R.K., 2004. Preferential accumulation of microbial carbon in aggregate structures of no-tillage soils. *Soil Sci. Soc. Am. J.* 68, 1249–1255.
- Six, J., Frey, S.D., Thiet, R.K., Batten, K.M., 2006. Bacterial and fungal contributions to carbon sequestration in agroecosystems. *Soil Sci. Soc. Am. J.* 70, 555–569.
- Sollins, P., Swanston, C., Kleber, M., Filley, T., Kramer, M., Crow, S., Caldwell, B.A., Lajtha, K., Bowden, R., 2006. Organic C and N stabilization in a forest soil: Evidence from sequential density fractionation. *Soil Biol. Biochem.* 38, 3313–3324.
- Stumm, W., 1997. Reactivity at the mineral-water interface: Dissolution and inhibition. *Colloids Surf. A Physicochem. Eng. Asp.* 120, 143–166.
- Thevenot, M., Dignac, M.F., Rumpel, C., 2010. Fate of lignins in soils: A review. *Soil Biol. Biochem.* 42, 1200–1211.
- Tian, D.S., Niu, S.L., 2015. A global analysis of soil acidification caused by nitrogen addition. *Environ. Res. Lett.* 10, 024019.
- Van Groenigen, K.-J., Six, J., Harris, D., Van Kessel, C., 2007. Elevated CO₂ does not favor a fungal decomposition pathway. *Soil Biol. Biochem.* 39, 2168–2172.
- Vance, E.D., Brookes, P.C., Jenkinson, D.S., 1987. An extraction method for measuring soil microbial biomass-C. *Soil Biol. Biochem.* 19, 703–707.
- Vitousek, P.M., Porder, S., Houlton, B.Z., Chadwick, O.A., 2010. Terrestrial phosphorus limitation: mechanisms, implications, and nitrogen-phosphorus interactions. *Ecol. Appl.* 20, 5–15.
- Wang, B.R., An, S.S., Liang, C., Liu, Y., Kuzyakov, Y., 2021. Microbial necromass as the source of soil organic carbon in global ecosystems. *Soil Biol. Biochem.* 162, 108422.
- Wang, Y., Lv, W., Xue, K., Wang, S., Zhang, L., Hu, R., Zeng, H., Xu, X., Li, Y., Jiang, L., Hao, Y., Du, J., Sun, J., Dorji, T., Piao, S., Wang, C., Luo, C., Zhang, Z., Chang, X., Zhang, M., Hu, Y., Wu, T., Wang, J., Li, B., Liu, P., Zhou, Y., Wang, A., Dong, S., Zhang, X., Gao, Q., Zhou, H., Shen, M., Wilkes, A., Mische, G., Zhao, X., Niu, H., 2022b. Grassland changes and adaptive management on the Qinghai-Tibetan Plateau. *Nat. Rev. Earth Environ.* 3, 668–683.
- Wang, X., Wang, C., Cotrufo, M.F., Sun, L.F., Jiang, P., Liu, Z.P., Bai, E., 2020. Elevated temperature increases the accumulation of microbial necromass nitrogen in soil via increasing microbial turnover. *Global Change Biol.* 26, 5277–5289.
- Wang, Q.C., Yang, L.M., Song, G., Jin, S.S., Hu, H.W., Wu, F.Z., Zheng, Y., He, J.Z., 2022a. The accumulation of microbial residues and plant lignin phenols are more influenced by fertilization in young than mature subtropical forests. *For. Ecol. Manage.* 509, 102074.
- Widdig, M., Heintz-Buschart, A., Schleuss, P.M., Guhr, A., Borer, E.T., Seabloom, E.W., Spohn, M., 2020. Effects of nitrogen and phosphorus addition on microbial community composition and element cycling in a grassland soil. *Soil Biol. Biochem.* 151, 108041.
- Wieder, W.R., Cleveland, C.C., Smith, W.K., Todd-Brown, K., 2015. Future productivity and carbon storage limited by terrestrial nutrient availability. *Nat. Geosci.* 8, 441–444.
- Wilpiseski, R.L., Aufrecht, J.A., Retterer, S.T., Sullivan, M.B., Graham, D.E., Pierce, E. M., Zablocki, O.D., Palumbo, A.V., Elias, D.A., 2019. Soil Aggregate Microbial Communities: Towards Understanding Microbiome Interactions at Biologically Relevant Scales. *Appl. Environ. Microbiol.* 85, e00324–e00419.
- WRB, I.W.G., 2015. World reference base for soil resources 2014, update 2015: International soil classification system for naming soils and creating legends for soil maps. *World Soil Resources Reports No. 106*. FAO, Rome.
- Xu, B., Wang, J.N., Wu, N., Wu, Y., Shi, F.S., 2018. Seasonal and interannual dynamics of soil microbial biomass and available nitrogen in an alpine meadow in the eastern part of Qinghai-Tibet Plateau, China. *Biogeosciences* 15, 567–579.
- Yuan, Y., Li, Y., Mou, Z.J., Kuang, L.H., Wu, W.J., Zhang, J., Wang, F.M., Hui, D.F., Penuelas, J., Sardans, J., Lambers, H., Wang, J., Kuang, Y.W., Li, Z.A., Liu, Z.F., 2021. Phosphorus addition decreases microbial residual contribution to soil organic carbon pool in a tropical coastal forest. *Global Change Biol.* 27, 454–466.
- Yue, K., Fornara, D.A., Yang, W.Q., Peng, Y., Peng, C.H., Liu, Z.L., Wu, F.Z., 2017. Influence of multiple global change drivers on terrestrial carbon storage: additive effects are common. *Ecol. Lett.* 20, 663–672.
- Zhang, X., Amelung, W., 1996. Gas chromatographic determination of muramic acid, glucosamine, mannosamine, and galactosamine in soils. *Soil Biol. Biochem.* 28, 1201–1206.
- Zhang, X.Y., Jia, J., Chen, L.T., Chu, H.Y., He, J.S., Zhang, Y.J., Feng, X.J., 2021. Aridity and NPP constrain contribution of microbial necromass to soil organic carbon in the Qinghai-Tibet alpine grasslands. *Soil Biol. Biochem.* 156, 108213.
- Zhang, J.Y., Zhang, N., Liu, Y.X., Zhang, X.N., Hu, B., Qin, Y., Xu, H.R., Wang, H., Guo, X. X., Qian, J.M., Wang, W., Zhang, P.F., Jin, T., Chu, C.C., Bai, Y., 2018. Root microbiota shift in rice correlates with resident time in the field and developmental stage. *Sci. China-Life Sci.* 61, 613–621.
- Zhu, E.X., Cao, Z.J., Jia, J., Liu, C.Z., Zhang, Z.H., Wang, H., Dai, G.H., He, J.S., Feng, X. J., 2021. Inactive and inefficient: Warming and drought effect on microbial carbon processing in alpine grassland at depth. *Global Change Biol.* 27, 2241–2253.
- Zhu, S.S., Dai, G.H., Ma, T., Chen, L.T., Chen, D.M., Lu, X.T., Wang, X.B., Zhu, J.T., Zhang, Y.J., Bai, Y.F., Han, X.G., He, J.S., Feng, X.J., 2019. Distribution of lignin phenols in comparison with plant-derived lipids in the alpine versus temperate grassland soils. *Plant Soil* 439, 325–338.
- Zhu, X.F., Jackson, R.D., DeLucia, E.H., Tiedje, J.M., Liang, C., 2020. The soil microbial carbon pump: From conceptual insights to empirical assessments. *Global Change Biol.* 26, 6032–6039.